

*promoting access to White Rose research papers*



**Universities of Leeds, Sheffield and York**  
**<http://eprints.whiterose.ac.uk/>**

---

This is an author produced version of a paper published in **IEEE Journal of Quantum Electronics**.

White Rose Research Online URL for this paper:  
<http://eprints.whiterose.ac.uk/42884>

---

**Published paper**

Vines, P. ,Tan, C.H., David, J.P.R., Attaluri, R.S., Vandervelde, T.E., Krishna, S., Jang, W.Y., Hayat, M.M. (2011) *Versatile spectral imaging with an algorithm-based spectrometer using highly tuneable quantum dot infrared photodetectors*, IEEE Journal of Quantum Electronics, 47 (2), pp. 190-197

<http://dx.doi.org/10.1109/JQE.2010.2065216>

---

# Versatile Spectral Imaging With an Algorithm-Based Spectrometer Using Highly Tuneable Quantum Dot Infrared Photodetectors

Peter Vines, Chee Hing Tan, John P. R. David, Ram S. Attaluri, Thomas E. Vandervelde, Sanjay Krishna, Woo-Yong Jang, and Majeed M. Hayat

**Abstract**— We report on the implementation of an algorithm-based spectrometer [Sakoğlu et al., *Applied Optics*, 4(28), 7224-7234, 2006] capable of reconstructing the spectral shape of materials in the MWIR and LWIR wavelengths using only experimental photocurrent measurements from quantum dot infrared photodetectors (QDIPs). The algorithm theory and implementation will be described, followed by an investigation into this algorithmic spectrometer's performance. Compared to the QDIPs utilized in an earlier implementation, the QDIPs used have highly varying spectral shapes and four spectral peaks across the MWIR and LWIR wavelengths. It has been found that the spectrometer is capable of reconstructing broad spectral features of a range of band pass infrared filters between wavelengths of  $4\mu\text{m}$  and  $12\mu\text{m}$  as well as identifying absorption features as narrow as  $0.3\mu\text{m}$  in the IR spectrum of a polyethylene sheet.

**Index Terms**— Algorithmic spectrometer, hyperspectral imaging, multispectral imaging, quantum dot infrared photodetectors.

## I. INTRODUCTION

MULTISPECTRAL and hyperspectral imaging in the mid-wave infrared (MWIR) and long-wave infrared (LWIR) regions has attracted much interest due to a wide

Manuscript received March 10, 2010. This work was supported by the Electro-Magnetic Remote Sensing (EMRS) Defence Technology Centre, established by the UK Ministry of Defence and run by a consortium SELEX Sensors and Airborne Systems, Thales Defence, Roke Manor Research and Filtronic (ref. EMRS/DTC/7/169) and the UK Ministry of Defence Competition of Ideas (ref. A1471). Additional support was received from the National Consortium from the MASINT Research (NCOM) Partnership Project (USA) and the National Science Foundation (USA).

P. Vines, C. H. Tan and J. P. R. David are with the Department of Electronic and Electrical Engineering, University of Sheffield, Sheffield, S1 3JD, U.K. (e-mail: elp05pv@sheffield.ac.uk, c.h.tan@sheffield.ac.uk, j.p.david@sheffield.ac.uk).

S. Krishna, W. Y. Jang and M. M. Hayat are with the Department of Electrical and Computer Engineering and Center for High Technology Materials, University of New Mexico, Albuquerque, New Mexico, NM 87131-1356, U.S.A.

R. S. Attaluri was with Department of Electrical and Computer Engineering and Center for High Technology Materials, University of New Mexico, Albuquerque, New Mexico, NM 87131-1356, U.S.A. He is now with Lehigh University, Bethlehem, PA 18015 USA

T. E. Vandervelde was with the Department of Electrical and Computer Engineering and the Center for High Technology Materials, University of New Mexico, Albuquerque, NM 87131-1356 USA. He is now with Tufts University, Medford, MA 02155 USA.

range of applications in areas such as advanced reconnaissance, chemical sensing and atmospheric pollutant gas monitoring. Presently multispectral imagers use optical filter wheels to filter radiation incident on a wideband infrared (IR) detector [1]. The filters require cooling to prevent additional IR emission which makes these systems operationally costly as well as bulky. Hyperspectral imagers use dispersive scanning optics to diffract the IR radiation and also use a wideband, panchromatic detector [2], [3]. These moving parts cause the system to be less reliable, bulky and more costly than purely electronic imagers. To achieve multicolor detection, a multi-junction Cadmium Mercury Telluride (CdHgTe) detector, with varying Cd compositions, has been adopted [4]. A similar approach to grow quantum well infrared photodetectors (QWIPs) with four spectral bands has also been demonstrated [5]. Achieving a high number of wavelength bands using this approach is difficult.

A novel flexible imaging technique has been proposed [6] as an alternative to these technologies. An algorithm combines the responses of a number of spectrally different detectors or a range of varied responses from a single detector using predetermined weighting factors to calculate the incident radiation as a function of wavelength across a specified wavelength range. Since this algorithmic spectrometer system can be pre-programmed with a specific spectral resolution and IR wavelength range it can be highly flexible and the absence of any optical filters or scanning optics makes the system potentially compact, cheap and reliable. If the algorithmic spectrometer can operate with a single type of detector – one with a varying spectral response – the effective pixel area on 2D multispectral focal plane arrays (FPA) can be increased without decreasing the spatial resolution of the FPA or altering the optical dimensions.

A number of detectors are in use in the MWIR and LWIR wavelength range. Well established narrow bandgap CdHgTe based detectors can detect a wide IR wavelength region [7], however this range is usually fixed meaning a number of different structures would be required. QWIPs can be designed to exhibit a voltage tuneable spectral response [5]. However the wavelength range covered is usually small and hence is not ideal for the system described above, although in principle different quantum well designs can be adopted to yield the desired spectral characteristics. By incorporating

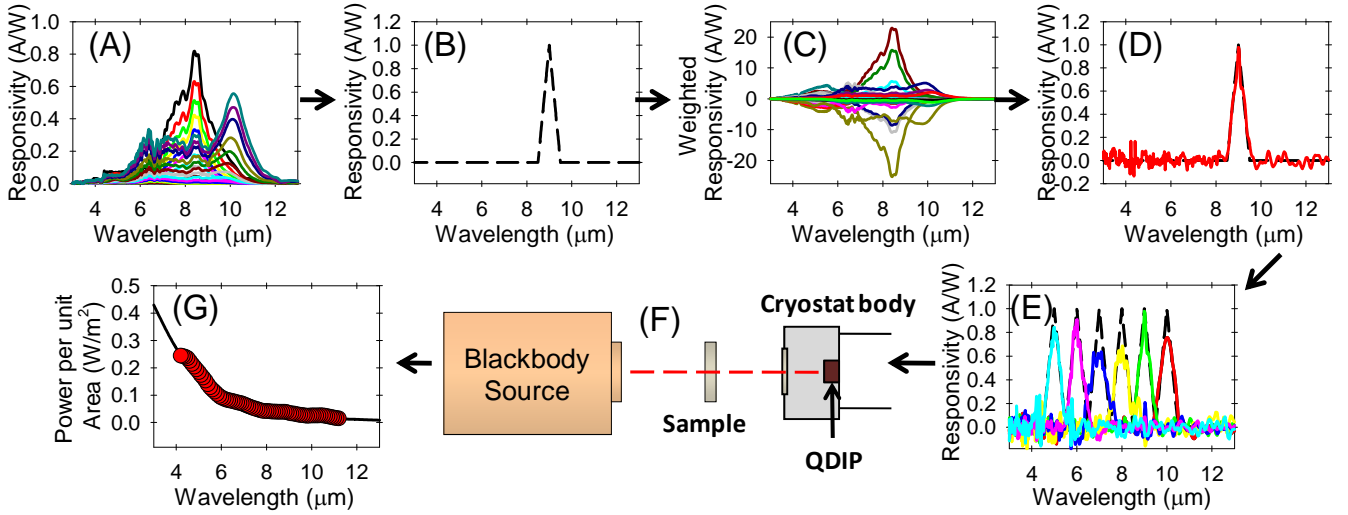


Fig. 1. Flow chart describing algorithmic spectrometer process. (A) Intrinsic QDIP responses at various applied bias voltages. (B) Desired arbitrary spectral shape – a narrow triangular bandpass filter. (C) Weighted intrinsic QDIP responses formed from multiplying the intrinsic QDIP responses by the associated weighting factors. (D) Sum of weighted intrinsic QDIP responses approximating desired triangular bandpass filter. (E) Approximations of desired triangular bandpass filters with different centre wavelengths. (F) Photocurrent measurement set-up. (G) Final reconstruction of incident unfiltered blackbody radiation.

quantum dots in the quantum wells, dot-in-a-well (DWELL) quantum dot infrared photodetectors (QDIPs) can be designed to exhibit a spectral response that can be tuned across a wide wavelength range [8], [9], as well as providing normal incidence detection. The spectral response of these detectors will vary as a function of the bias voltage applied across the detector allowing one QDIP to effectively act as several separate detectors with differing spectral responses.

Sakoğlu *et al.* [6] have shown that the varying spectral response of DWELL QDIPs can be combined with the algorithmic spectrometer technique for multispectral or hyperspectral imaging. The paper reported that the spectrometer was able to reconstruct the smooth spectral shape of blackbody radiation using theoretically estimated photocurrents. The algorithm has since been extended to include a signal to noise (SNR) term to increase the spectrometer's robustness to photocurrent measurement noise [10]. Recently the algorithmic spectrometer has been used successfully to reconstruct the spectra of bandpass filters in the LWIR region from experimental photocurrent measurements [11].

Previous demonstrations of the algorithmic spectrometer have used QDIPs with spectral responses that have not been ideal for this purpose. In this paper we will demonstrate the implementation of the spectrometer using more suitable QDIPs with highly variable spectral responses covering a broad IR wavelength range for imaging in both the MWIR and LWIR regions. The technique will be demonstrated at 77K whereas previously most accurate reconstructions have been achieved at 30K. We have been able to use this technique to capture narrow spectral features as well as the broad envelope of incident radiation over a wavelength range that is twice as great as previously achieved. Section 2 reviews the algorithmic spectrometer technique in more detail with section 3 detailing the structure and characteristics of the

QDIPs used and section 4 presenting results obtained using the algorithmic spectrometer.

## II. ALGORITHMIC SPECTROMETER THEORY

The algorithmic spectrometer theory is described fully elsewhere [10], hence an overview of the system will be provided here with the process detailed in fig. 1. The spectrometer works on the principle that by summing the weighted spectral responses from any given number of bias voltages for a single QDIP, a desired arbitrary spectral shape can be approximated. For hyperspectral or multispectral imaging purposes this spectral shape can take the form of a bandpass filter (with the triangular shape illustrated in fig. 1B, for example), therefore allowing a number of potentially wideband intrinsic responses from the detectors (as shown in fig. 1A) to be combined to form an approximated narrowband response (as shown in figs. 1D and 1E).

The algorithm approximates a desired spectral shape with an optimized, least mean square error (MSE) fit by calculating a set of weighting factors with each weighting factor corresponding to the spectral response at a specific bias voltage.

$$\mathbf{w} = (\mathbf{A}^T \mathbf{A} + \Phi)^{-1} \mathbf{A}^T \mathbf{R} \quad (1)$$

where

$$\mathbf{A} = \begin{bmatrix} R_{V_1}(\lambda_1) & R_{V_2}(\lambda_1) & \dots & R_{V_M}(\lambda_1) \\ R_{V_1}(\lambda_2) & R_{V_2}(\lambda_2) & \dots & R_{V_M}(\lambda_2) \\ \vdots & \vdots & \vdots & \vdots \\ R_{V_1}(\lambda_L) & R_{V_2}(\lambda_L) & \dots & R_{V_M}(\lambda_L) \end{bmatrix} \quad (2)$$

and

$$\mathbf{R} = \begin{bmatrix} R(\lambda_1) \\ R(\lambda_2) \\ \vdots \\ R(\lambda_L) \end{bmatrix} \quad (3)$$

The weighting factors are calculated using (1) where  $\mathbf{w}$  is the weight vector corresponding to the set of weighting factors at each bias voltage (for measurements at  $M$  bias voltages a set of weights  $w_1, w_2, \dots, w_M$  will exist),  $\mathbf{A}$  is the matrix formed by the intrinsic QDIP responsivities as a function of wavelength and applied bias voltage as shown in (2) and  $\mathbf{R}$  is the desired arbitrary spectral shape as a function of wavelength shown in (3). The SNR term,  $\Phi$ , is described below, for ideal noiseless measurements it is a zero matrix.

In the reconstructions presented in this paper,  $\mathbf{R}$  takes the form of a narrow, triangular bandpass filter since it was found that the algorithmic spectrometer could produce better fits to this shape in a MSE sense when compared to the fits to the Gaussian or rectangular filter shapes which were trialed. The size of  $\mathbf{A}$  is equal to  $V \times \lambda$  where  $V$  is the number of bias voltages used by the spectrometer in the reconstruction and  $\lambda$  is the number of discrete responsivity readings in the wavelength range for both the intrinsic QDIP responsivities and the desired narrow, triangular bandpass filters. The size of  $\mathbf{A}$  varies from  $4 \times 1001$  to  $31 \times 1001$  in this work.

Equation (1) can be calculated for any number of desired narrow, triangular bandpass filters with differing centre wavelengths across the wavelength range of interest, each bandpass filter will have its own specific set of weighting factors, thus providing the spectroscopy measurement capability.

Photocurrent measurements can then be taken when the device is exposed to radiation from an object of interest. The incident power per unit area per unit wavelength at a specific wavelength,  $\lambda_c$ , can be approximated by taking the predetermined set of weights for the bandpass filter with centre wavelength,  $\lambda_c$ , and summing the products of the photocurrent at each bias voltage and the corresponding weighting factor at that bias voltage. This is shown in (4) where  $I_{V_1}, \dots, I_{V_M}$  is the photocurrent at a specific bias voltage,  $w_{V_i, \lambda_c}$  is the weight for a specific bias voltage and centre wavelength and  $D_c$  relates the sum of the weighted photocurrents to the reconstructed incident power and is equal to the peak responsivity of the desired bandpass filter multiplied by the full width half maximum (FWHM) of the desired bandpass filter.

$$P_C = \frac{\sum_{i=1}^M w_{V_i, \lambda_c} I_{V_i}}{D_c} \quad (4)$$

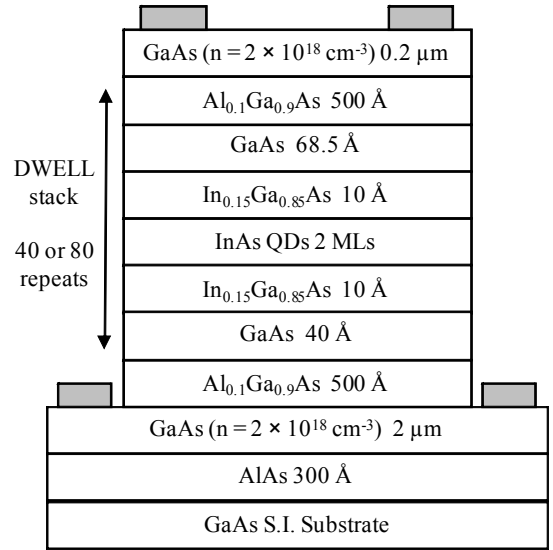


Fig. 2. Structure of the QDIPs used in this work to evaluate the algorithmic spectrometer theory.

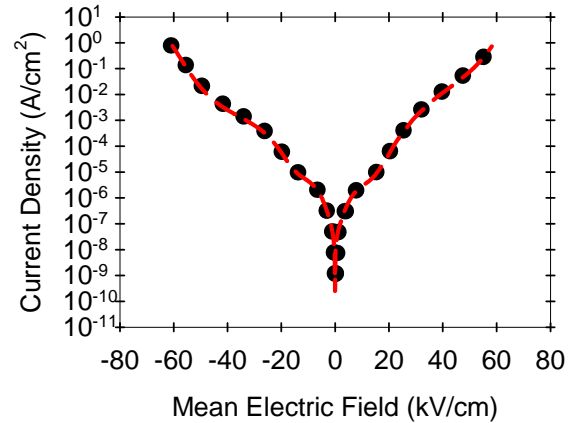


Fig. 3. Dark current at 77K as a function of mean electric field for the 40 stack (black dotted line) and 80 stack (red dashed line) QDIPs.

The SNR term,  $\Phi$ , included in equation 1 can be incorporated into the algorithm to decrease the spectrometer's sensitivity to noise in the photocurrent measurements [10], arising from the equipment, background and the detector. This has the effect of reducing the magnitude of the weighting factors and therefore reducing the accumulation of noise in the summation.

It is also possible to include a regularization term in the algorithm to avoid any spurious fluctuations in the resultant approximated spectra generally originating from the intrinsic QDIP spectra [10]. However the QDIPs used in this work had strong intrinsic spectral responses which did not exhibit these fluctuations, it was therefore found that including the regularization term did not yield a significant improvement to the bandpass filter approximations and the resultant spectral reconstructions.

### III. QUANTUM DOT INFRARED PHOTODETECTORS

The structure of the two QDIPs used by the spectrometer in this work is shown in fig. 2. Either 40 or 80 DWELL stacks

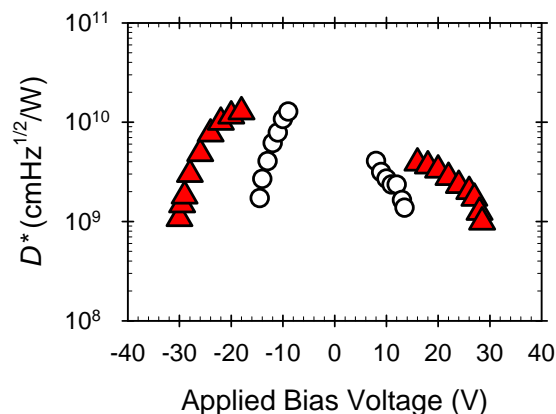


Fig. 4.  $D^*$  at 77K as a function of mean electric field for the 40 stack (open circles) and 80 stack (red triangles) QDIPs.

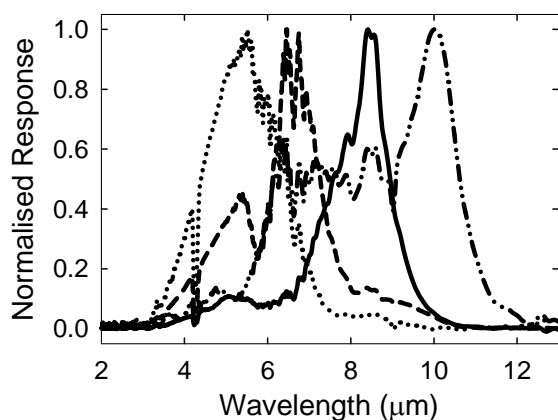


Fig. 5. Normalized spectral response at 77K for the 80 stack QDIP at applied bias voltages of -18V (solid line), -2V (dotted line), +10V (dashed line) and +24V (dot-dashed line).

were grown between two Si doped ( $2 \times 10^{18} \text{cm}^{-3}$ )  $n^+$  GaAs regions. Each DWELL stack consisted of quantum dots grown using 2.0 monolayers of InAs with Si doping concentration of  $1.4 \times 10^{11} \text{cm}^{-2}$ , giving approximately 1 electron/dot. The quantum dots are grown within a  $20 \text{\AA}$   $\text{In}_{0.15}\text{Ga}_{0.85}\text{As}$  well ( $10 \text{\AA}$  above the dot and  $10 \text{\AA}$  below) which in turn is situated in a  $108.5 \text{\AA}$  GaAs well ( $68.5 \text{\AA}$  and  $40 \text{\AA}$  below).  $500 \text{\AA}$   $\text{Al}_{0.1}\text{Ga}_{0.9}\text{As}$  barriers separated the DWELL regions. The wafers were fabricated using standard GaAs wet chemical processing techniques into circular mesa diodes with diameters of  $200 \mu\text{m}$  and  $400 \mu\text{m}$  and packaged using standard TO5 headers.

Dark current measurements were undertaken on both QDIPs at temperatures from 20K to 290K as reported in other work [12], [13]. Fig. 3 shows that the dark current was constant between the two devices at a specific temperature and mean electric field (calculated by dividing the applied bias voltage by the intrinsic region width). Two important observations can be drawn from these results. First, no degradation in the dark current was observed with growth of up to 80 DWELL stacks indicating highly uniform growth of the QD layers and the absence of strain accumulation in these devices and secondly the desired operating voltage can be obtained by selecting appropriate number of DWELL stacks.

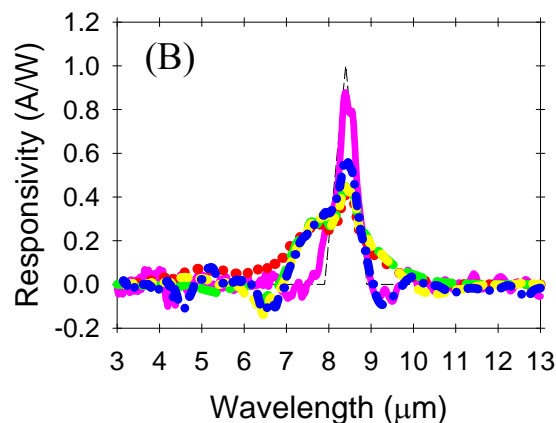
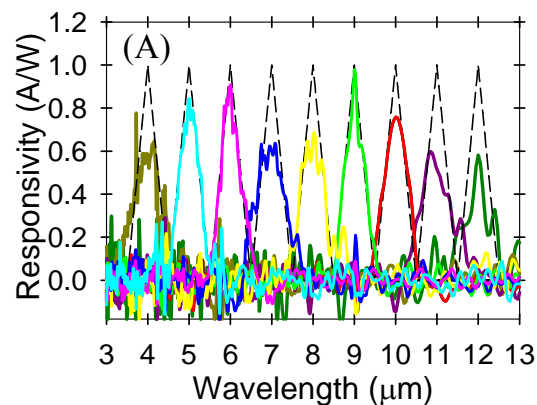


Fig. 6. (A) Triangular bandpass filter approximations (solid color lines) with FWHM of  $0.5 \mu\text{m}$  formed from 31 QDIP spectra with centre wavelengths ranging from  $4.0 \mu\text{m}$  to  $12.0 \mu\text{m}$  shown against the desired triangular bandpass filters (dashed black lines). (B) Fitting to a desired triangular bandpass filter with a FWHM of  $0.5 \mu\text{m}$  and a centre wavelength of  $8.4 \mu\text{m}$  (dashed black line) using intrinsic QDIP spectra from 1 (red dotted line), 2 (green long dashed line), 4 (yellow short dashed line), 6 (blue dot-dashed line) and 31 (pink solid line) bias voltages.

Responsivity and noise current measurements at 77K were used to calculate the detectivity,  $D^*$ , in these devices as shown in fig. 4.  $D^*$  is effectively constant between the two QDIPs for a given mean electric field confirming the highly uniform growth. The high  $D^*$  exhibited is important since it enables the algorithmic spectrometer to image with a narrow spectral resolution using larger weighting factors, allowing narrow spectral features to be reconstructed and allowing imaging at a higher temperature than previously achieved.

The QDIP's spectral response was measured at 77K using a Varian 7000 FTIR Spectrometer. It was found that the spectral response at any given mean electric field was identical between the two QDIPs confirming the uniform growth for the two structures.

Fig. 5 shows that the spectral response in the 80 stack QDIP varies significantly across the bias voltage range. The peak absorption wavelength was found to shift from  $5.5 \mu\text{m}$  at -2V to  $10 \mu\text{m}$  at 24V. It is this spectral diversity that makes these QDIPs ideally suited for use with the algorithmic spectrometer. Note that significantly higher applied bias voltages are possible in our QDIPs compared to those used in previous works [6], [10], [11] due to the thick intrinsic regions

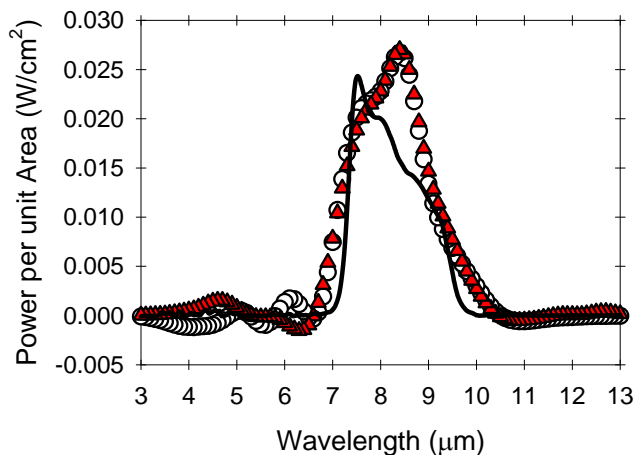


Fig. 7. LWIR filter spectrum (solid black line) reconstructed with 31 bias voltages (open circles) or 4 bias voltages (red triangles) and using triangular bandpass filters with FWHM of  $0.5\mu\text{m}$ .

of  $5.08\mu\text{m}$  and  $2.56\mu\text{m}$  for the 80 stack and 40 stack QDIPs respectively.

Fig. 6(A) shows that this spectral variation can be exploited by the algorithm to give excellent approximations to desired triangular bandpass filters with peak wavelengths ranging from  $12.0\mu\text{m}$  to  $4.0\mu\text{m}$  and a FWHM of  $0.5\mu\text{m}$ . A total of 31 different intrinsic spectral responses at bias voltages ranging from  $-29.5\text{V}$  to  $+28\text{V}$  were used in these approximations, with the resultant fits suitable to be used in reconstructing spectra with ideal noiseless photocurrent measurements. Note that the fitting is strongest between 5 and  $10\mu\text{m}$  – where the QDIP’s responsivity is also strongest. Where the QDIP’s responsivity is weaker – above  $10\mu\text{m}$  and below  $5\mu\text{m}$  – the approximations degrade in quality slightly but are still clearly identifiable. The noise floor in the reconstructed responsivities is due to incomplete removal of responses outside the approximated filters’ wavelengths. Fig. 6(B) shows that if the number of spectra used in the approximation is reduced then the MSE in the approximation increases although this is offset by a decrease in the time required to capture a single hyperspectral or multispectral image due to the reduced number of photocurrent measurements required. Therefore it is important to optimize the algorithm to determine the smallest number of measurements required to yield a satisfactory reconstruction of the desired spectral shape, as discussed in more detail in the following section.

#### IV. ALGORITHMIC SPECTROMETER EVALUATION

We will first examine the performance of the algorithmic spectrometer in the LWIR region. The algorithmic spectrometer was used to reconstruct a LWIR bandpass filter with cut-off wavelengths of  $7.1\mu\text{m}$  and  $9.7\mu\text{m}$ . The filter was placed between a blackbody source at a temperature of  $800^\circ\text{C}$  and the QDIP to form the spectrum shown in fig. 7. Photocurrent measurements were taken using the QDIP with 80 DWELL stacks at 31 different bias voltages from  $-29.5\text{V}$  to  $+28\text{V}$ .

It was found that the spectrometer could easily reconstruct

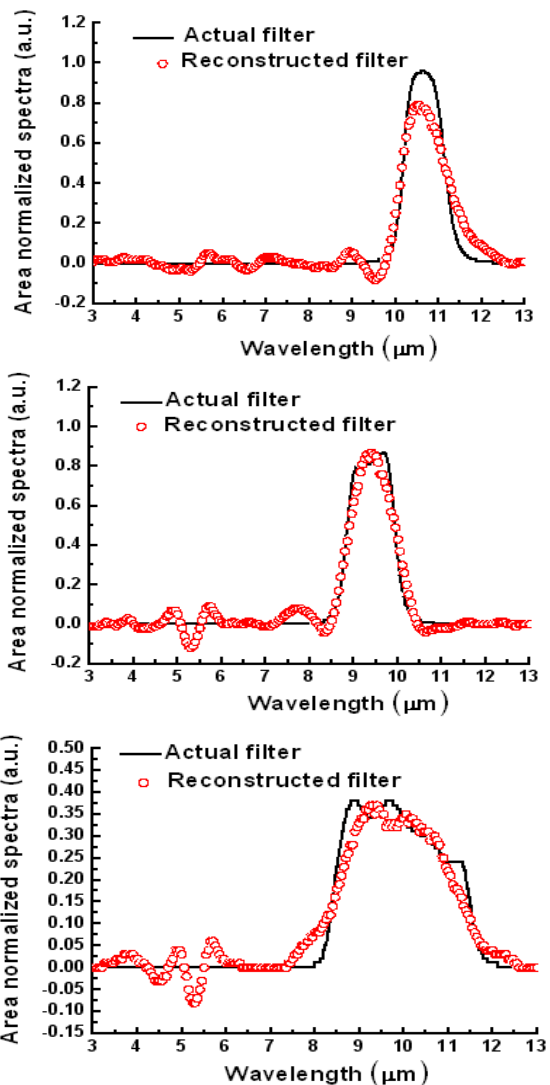


Fig. 8. Three LWIR bandpass filters spectra (solid black lines) reconstructed using 31 bias voltages and triangular bandpass filters with FWHM of  $0.5\mu\text{m}$  (red open circles).

the LWIR filter spectrum, fig. 7 shows that the algorithmic spectrometer is able to reconstruct the filter characteristics using 31 bias voltages and triangular bandpass filters with FWHM of  $0.5\mu\text{m}$ . Further analysis shows that excellent reconstructions can be achieved using as few as four bias voltages, allowing for a very short radiation capture time. This is due to the strong intrinsic response of the QDIPs in the  $7\text{--}10\mu\text{m}$  range. The discrepancy around  $8\text{--}9\mu\text{m}$  is caused by errors in accurately approximating the triangular bandpass filters. Note that the MSE of these filters is higher than those depicted in fig 6A since in this case the algorithm has been made robust to photocurrent measurement noise. Although this SNR in the measured photocurrent is accounted for in the calculations of the weighting factors, this results in a higher error in the reconstruction of the target spectrum compared with an ideal reconstruction using theoretical noiseless photocurrent measurements due to the overestimation of the triangular filters in the  $8\text{--}9\mu\text{m}$  range. The discrepancy could

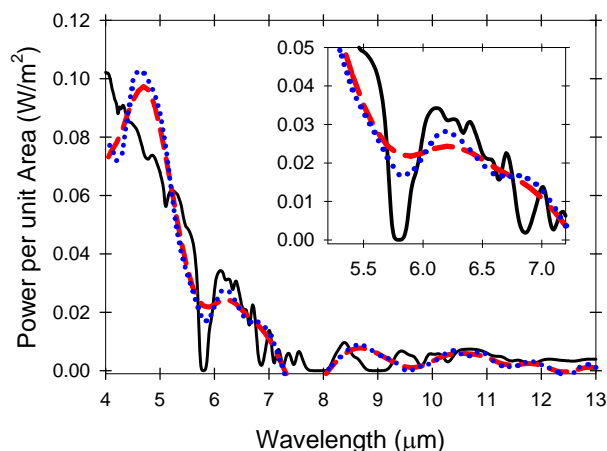


Fig. 9. Polyethylene sheet spectrum (black solid line) reconstructed with the algorithmic spectrometer using 27 bias voltages and a triangular band pass filter FWHM of  $0.5\mu\text{m}$  (red dashed line) or  $0.25\mu\text{m}$  (blue dotted line). Inset is enlarged around the absorption feature at  $5.8\mu\text{m}$ .

be reduced by improving the SNR in the photocurrent measurements thereby allowing more accurate bandpass filter approximations.

Selecting the optimum combination and number of bias voltages is dependent on the variation of the QDIP's spectral response across the wavelength range. When the number of bias voltages selected out of the possible 31 is greater than three it is prohibitively time consuming to test the spectrometer with each combination due to the large number of combinations. For instance if the spectrometer selects any 4 bias voltages out of a possible 31 then there are over 31000 different combinations, if any 6 biases are chosen there are  $\sim 730000$  combinations. A detailed analysis of the optimal number and selection of bias voltages is outside the scope of this paper; however our trials have shown us that an accurate reconstruction across the wavelength range depends on two major factors. Firstly it is essential that the combined intrinsic QDIP responses are strong across the wavelength range to be reconstructed, if areas of the spectrum are only covered by weak responses the reconstruction will also be weak in this area due to a poor approximation of the desired filters at this wavelength. Secondly the intrinsic responses must vary in shape across the bias range to allow the algorithm many opportunities to fit to the desired filters. Therefore the reconstructions achieved in this work have used a set of bias voltages which have intrinsic QDIP spectra which cover the wavelength range of interest and have a roughly uniform variation in spectral shape from one bias voltage to the next.

Three further LWIR filters were used to demonstrate the versatility of the algorithmic spectrometer, as shown in fig. 8. In these examples 31 bias voltages from the QDIP with 80 stacks were used, with photocurrents calculated from the product of the QDIP's responsivity and the incident radiation. The three bandpass filters had cutoff wavelengths of  $8.2\text{--}11.8\mu\text{m}$ ,  $8.5\text{--}10.2\mu\text{m}$  and  $10.0\text{--}11.5\mu\text{m}$ . In reconstructing these spectra the spectrometer has shown that it is capable of accurate reconstructions at wavelengths where the intrinsic response of the QDIP is relatively weak. The small

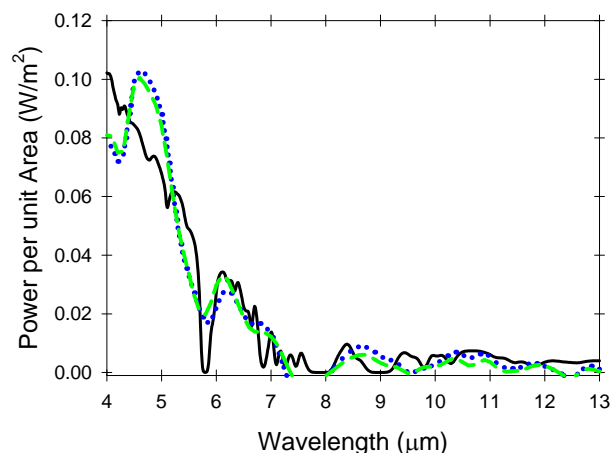


Fig. 10. Polyethylene sheet spectrum (black solid line) reconstructed with the algorithmic spectrometer using triangular bandpass filters with FWHM of  $0.25\mu\text{m}$  and using 27 bias voltages (blue dotted line) or 14 bias voltages (green dashed line).

oscillations away from the main peaks in the LWIR filter reconstructions are caused by small errors in the desired filter approximations associated with these wavelengths. These errors occur at wavelengths where incident radiation is present, causing the algorithm to attribute this incident radiation to wavelengths where it is not present.

The filters presented relatively simple spectra for the algorithmic spectrometer to reconstruct. A more stringent test using a polyethylene sheet was used to evaluate the spectrometers performance in the MWIR region. Polyethylene has a relatively strong transmission in the MWIR, where the intrinsic response of the QDIP is weak, and has a number of narrow spectral absorption features. It follows that a polyethylene sheet can be used to (i) examine the algorithmic spectrometer's performance in the MWIR and (ii) test the algorithmic spectrometer's capability in reconstructing narrow spectral features.

The photocurrent measurements were recorded with the polyethylene sheet placed between the QDIP and a blackbody source at a temperature of  $800^\circ\text{C}$  with the resultant incident spectra shown in fig. 9. The 40 DWELL stack QDIP was used in order to reduce the operating voltage and measurements were taken at 27 bias voltages from  $-14\text{V}$  to  $+13\text{V}$ .

Results of using 27 bias voltages and triangular bandpass filters with FWHM of  $0.5\mu\text{m}$  are shown in fig. 9, the absorption features at  $8\mu\text{m}$  and  $5.8\mu\text{m}$  are clearly indicated and the spectrometer gives a reasonably accurate reconstruction of the envelope of the power density.

Since the absorption feature at  $5.8\mu\text{m}$  has a narrower width ( $0.3\mu\text{m}$ ) than the triangular bandpass filter's FWHM ( $0.5\mu\text{m}$ ) it is challenging to capture it correctly. If the FWHM of the triangular bandpass filters are reduced it is possible to improve the reconstruction of narrow features. Fig. 9 also shows the polyethylene reconstruction using triangular bandpass filters with FWHM of  $0.25\mu\text{m}$ . The  $5.8\mu\text{m}$  feature is now more pronounced in the reconstruction. Reducing the FWHM of the bandpass filters below  $0.25\mu\text{m}$  does not produce any further improvements in the reconstruction due to

the poor approximation to very narrow bandpass filters. This is due to the need for larger weighting factors for approximations with very narrow FWHM which leads to an increase in the cumulative effect of measurement noise.

An attempt to minimize the number of bias voltages required to reconstruct the polyethylene spectrum was carried out. When the number of bias voltages is reduced to 14 the measurement time required to reconstruct the spectrum is approximately halved and fig. 10 shows that the quality of the reconstruction does not degrade. Since the 14 bias voltages can still cover the QDIP's intrinsic spectral shapes and peaks, the narrowband filter approximations do not alter significantly allowing the polyethylene spectrum to be reconstructed with a similar accuracy as with 27 biases. Reducing the number of bias voltages further gradually causes some of the QDIP's intrinsic spectral shapes to be lost and the resultant reconstruction degrades accordingly. However our results show that the algorithm-based spectrometer is a promising approach towards achieving a highly adaptable IR sensor.

Further improvements to the reconstruction are possible if the SNR can be increased. This will allow the narrow bandpass filters to be better approximated since, as the spectrometer does not need to be as robust to measurement noise, larger weighting factors may be used [10]. Decreasing the QDIP's operating temperature reduces the dark current and noise current and is therefore one way to achieve further improvement in the spectral reconstruction.

## V. CONCLUSION

The algorithmic spectrometer reported in [10] has been demonstrated at higher temperatures than previously reported using QDIPs with spectral responses which vary significantly with applied bias voltage. Spectrometer testing has shown that it is capable of reconstructing broad features in the 4-12 $\mu\text{m}$  region using few bias voltages allowing for a short radiation capture time. At present determining the minimum number of bias voltage to use as well as the combination of these measurements is not trivial. Our work suggests that selecting the spectral responses which differ significantly in spectral shape and together cover a large wavelength range will provide the best set of data to be used during the reconstruction. It has been possible to capture spectral features as narrow as 0.3 $\mu\text{m}$  using desired triangular bandpass filters with a FWHM of a similar magnitude. Although the QDIPs used at present have operating voltages that are too high for FPA integration they would be ideal for single-pixel applications, furthermore it should be possible to reduce the intrinsic width of the QDIPs to give an FPA suitable detector. Extensive testing and evaluation will insure that an application-specific optimal system can reconstruct unknown targets with the shortest possible capture time over the specified wavelength range required and with the specified spectral resolution, and will allow the spectrometer reconstruction accuracy to be quantified. While we have achieved encouraging results using a fairly simple algorithm,

further developments including improvements the QDIP designs with wider spectral tunability and improvements to the algorithm could lead to a new class of multi/hyperspectral imaging on the chip capability.

## REFERENCES

- [1] L. G. Hipwood, I. M. Baker, C. L. Jones, C. Maxey, H. W. Lau, J. Fitzmaurice, M. Wilson, and P. Knowles, "LW IRFPAs made from HgCdTe grown by MOVPE for use in multispectral imaging" in *Proc. SPIE*, Infrared technology and applications, 2008, vol. 6940, p. 69400G.
- [2] N. Gupta, and D. Smith, "A field-portable simultaneous dual-band infrared hyperspectral imager". in *Proc. AIPR*, 2005, pp. 87–92
- [3] M. Hinrichs, and N. Gupta, "Comparison of QWIP to HgCdTe detectors for gas imaging" in *Proc. SPIE*, Infrared Technology and Applications, 2008, vol. 6940, p. 69401Q.
- [4] L. G. Hipwood, C. L. Jones, C. D. Maxey, H. W. Lau, J. Fitzmaurice, R. A. Catchpole, and M. Ordish "Three-color MOVPE MCT diodes" in *Proc. SPIE*, Infrared technology and applications, 2006, vol. 6206, p. 20612.
- [5] S. D. Gunapala, S. V. Bandara, J. K. Liu, S. B. Rafol, and J. M. Mumolo, "640 $\times$ 512 pixel long-wavelength infrared narrowband, multiband, and broadband QWIP focal plane arrays", *IEEE Trans. Electron Devices*, vol. 50 no. 12, pp. 2353–2360, Dec. 2003.
- [6] Ü. Sakoğlu, J. S. Tyo, M. M. Hayat, S. Raghavan, and S. Krishna, "Spectrally adaptive infrared photodetectors with bias-tunable quantum dots", *J. Opt. Soc. Am. B*, vol. 21, no. 1, pp. 7–17, Jan. 2004.
- [7] J. Beck, C. Wan, M. Kinch, J. Robinson, P. Mitra, R. Scritchfield, F. Ma, and J. Campbell, "The HgCdTe electron avalanche photodiode", *J. Electron. Mater.*, vol. 35, no.6, pp. 1166–1173, 2006.
- [8] S. Raghavan, P. Rotella, A. Stintz, B. Fuchs, S. Krishna, C. Morath, D.A. Cardimona, and S.W. Kennerly, "High-responsivity, normal-incidence long-wave infrared ( $\lambda \sim 7.2\mu\text{m}$ ) InAs/In<sub>0.15</sub>Ga<sub>0.85</sub>As dots-in-a-well detector", *Appl. Phys. Lett.*, vol. 81, no. 8, pp. 1369–1371, Aug. 2002.
- [9] S. Krishna, S. Raghavan, G. von Winkel, A. Stintz, G. Ariyawansa, S. G. Matsik, and A. G. U. Perera, "Three-color ( $\lambda_{p1} \sim 3.8\mu\text{m}$ ,  $\lambda_{p2} \sim 8.5\mu\text{m}$ ,  $\lambda_{p3} \sim 23.2\mu\text{m}$ ) InAs/InGaAs quantum-dots-in-a-well detector", *Appl. Phys. Lett.*, vol. 83, no. 14, pp. 2745–2747, Oct. 2003.
- [10] Ü. Sakoğlu, M. M. Hayat, J. S. Tyo, P. Dowd, S. Annamalai, K. T. Posani, and S. Krishna "Statistical adaptive sensing by detectors with spectrally overlapping bands", *Appl. Opt.*, vol. 45, no 28, pp. 7224–7234, Oct. 2006.
- [11] W.-Y. Jang, M. M. Hayat, J. S. Tyo, R. S. Attaluri, T. E. Vandervelde, Y. D. Sharma, R. Sheno, A. Stintz, E. R. Cantwell, S. C. Bender, S. J. Lee, S. K. Noh, and S. Krishna, "Demonstration of bias-controlled algorithmic tuning of quantum dots in a well (DWELL) midIR detectors", *IEEE J. Quant. Electron.*, vol. 45, no. 6, pp. 674–683, Jun. 2009.
- [12] P. Vines, C. H. Tan, J. P. R. David, R. S. Attaluri, T. E. Vandervelde, and S. Krishna, "Noise, gain and responsivity in low strain quantum dot infrared photodetectors with up to 80 dot-in-a-well periods", in preparation for submission to *IEEE J. Quant. Electron.*
- [13] P. Vines, C. H. Tan, J. P. R. David, R. S. Attaluri, T. E. Vandervelde, and S. Krishna, "Multiple stack quantum dot infrared photodetectors" in *Proc. SPIE*, Electro-Optical and Infrared Systems: Technology and Applications, 2008, vol. 7113, p. 71130J.

**Peter Vines** (S'09) received the B.Eng. degree in electronic engineering from the University of Sheffield, Sheffield, U.K., in 2005, where he is currently working toward the Ph.D. degree in electronic and electrical engineering. His research interests include infrared detection and imaging using quantum dot infrared photodetectors and avalanche photodiodes.

**Chee Hing Tan** (M'95) received the B.Eng. and Ph.D. degrees in electronic engineering from the Department of Electronic and Electrical Engineering, University of Sheffield, Sheffield, U.K., in 1998 and 2002, respectively.

Since 2003, he has been with the Department of Electronic and Electrical Engineering, University of Sheffield, where he was earlier a Lecturer, and currently, a Senior Lecturer. He has extensive experience in characterization and modeling of high speed low noise avalanche photodiodes and phototransistors. His current research interests include single photon avalanche diodes, mid-infrared photodiodes, quantum dot infrared detectors, and ultrahigh speed avalanche photodiodes and phototransistors.

**John P. R. David** (SM'96) received the B.Eng. and Ph.D. degrees in electronic engineering from the University of Sheffield, Sheffield, U.K.

During 1985, he was with the Central Facility for III–V Semiconductors, Sheffield, where he was involved in the characterization activity. During 2001, he was with Marconi Optical Components (now Bookham Technologies). He is currently a Professor at the Department of Electronic and Electrical Engineering, University of Sheffield. His current research interests include piezoelectric III–V semiconductors and impact ionization in analogue and single-photon avalanche photodiodes.

Dr. David was an IEEE Lasers and Electro Optics Society (LEOS) Distinguished Lecturer from 2002 to 2004.

**Ram S. Attaluri** received the B.S. degree in computer engineering from the University of Madras, Chennai, India, and the M.S. and Ph.D. degrees in electrical engineering from the University of New Mexico, Albuquerque, in 2001 and 2007, respectively.

He is currently a Postdoctoral Research Associate in the Center for Optical Technologies, Lehigh University, Bethlehem, PA.



**Thomas E Vandervelde** (M'01) earned two B.S. degrees from the University of Massachusetts, Amherst, one in physics and the other in astronomy, both in 1999, his M.A. and Ph.D. degrees in Physics at the University of Virginia, Charlottesville, in 2001 and 2004, respectively.

He is the John Adams Endowed Chair Professor in the Electrical and Computer Engineering Department at Tufts University and Director of the Renewable Energy and Applied Photonics (REAP) Laboratories at Tufts University. He joined the faculty at Tufts in 2008. Prior to his present employment, he was a Research Assistant Professor at the Center for High Technology Materials at the University of New Mexico and a Post-Doctoral Fellow at University of New Mexico with Sanjay Krishna in 2007, University of Illinois Urbana-Champaign with Milton Feng in 2005-6, and University of Virginia with Michael Skrutskie in 2004-5. Additionally, he also was a Visiting Assistant Professor of Physics at Washington and Lee University in 2004-5. He has authored/co-authored several book chapters, over 30 peer-reviewed journal articles, over 30 conference presentations, and has one provisional patent. His current and previous research interests are group IV and III-V materials for photodetectors, photovoltaics/thermophotovoltaics, nanophysics/devices, and hetero-integrated circuits.

Prof. Vandervelde was recently on the executive committee for the local IEEE LEOS chapter in Albuquerque and in addition to IEEE and IEEE-LEOS, he is a member of APS, SPS, AAS, Eta Kappa Nu, Sigma Xi, MRS, TMS, AVS, and AAAS.

**Sanjay Krishna** received the Master's degree in physics from the Indian Institute of Technology (IIT), Madras, India, in 1996, the M.S. degree in

electrical engineering and the Ph.D. degree in applied physics from the University of Michigan, Ann Arbor, in 1999 and 2001, respectively.

He is the Associate Director of the Center for High Technology Materials and a Professor of electrical and computer engineering at the University of New Mexico. He joined the University of New Mexico as a tenure track faculty member in 2001. His present research interests include growth, fabrication and characterization of self-assembled quantum dots and type II InAs/InGaSb based strain layer superlattices for mid infrared detectors. He has authored/coauthored over 100 peer-reviewed journal articles, over 40 conference presentations, and two book chapters, and has five issued patents.

Dr. Krishna was a recipient of the Gold Medal from IIT, Madras, India, in 1996, the Best Student Paper Award at the 16th NAMBE Conference in Banff, Canada, in 1999, the 2002 Ralph E. Powe Junior Faculty Award from Oak Ridge Associated Universities, the 2003 IEEE Outstanding Engineering Award, 2004 Outstanding Researcher Award from the ECE Department, the 2005 School of Engineering Junior Faculty Teaching Excellence Award, the 2007 North American Molecular Beam Epitaxy Young Investigator Award, the 2007 NCMR-DIA Chief Scientist Award for Excellence, and the 2008 Early Career Achievement Award from the SPIE and the IEEE Nanotechnology Council. He was named the 2009 UNM Regents Lecturer and received the 2010 UNM Teacher of the Year Award.

**Woo-Yong Jang** received the B.E. degree in electrical engineering from the University of Canterbury, Christchurch, New Zealand, in 2001, and the M.S. degree in electrical engineering from the University of Southern California, Los Angeles, in 2004. He is currently working toward the Ph.D. degree in electrical and computer engineering at the University of New Mexico, Albuquerque.

He is currently a graduate student at the Center for High Technology Materials, University of New Mexico.

**Majeed M. Hayat** (S'89–M'92–SM'00) was born in Kuwait in 1963. He received the B.S. degree (*summa cum laude*) in electrical engineering from the University of the Pacific, Stockton, CA, in 1985, and the M.S. and Ph.D. degrees in electrical and computer engineering from the University of Wisconsin–Madison in 1988 and 1992, respectively. From 1993 to 1996, he was with the University of Wisconsin–Madison as a Research Associate and a Co-Principal Investigator of a project on statistical minefield modeling and detection, which was funded by the Office of Naval Research. In 1996, he joined the Faculty of the Electro-Optics Graduate Program and the Department of Electrical and Computer Engineering at the University of Dayton, Dayton, OH. He is currently a Professor in the Department of Electrical and Computer Engineering and the Center for High Technology Materials at the University of New Mexico, Albuquerque, NM. His research contributions cover a broad range of topics in the areas of statistical communication theory, optoelectronics, signal/image processing, remote sensing and applied probability theory. Specific research topics include avalanche photodiodes, optical communication systems, image restoration and enhancement, and queuing models for distributed computing systems and networks. Dr. Hayat is the recipient of the 1998 National Science Foundation Early Faculty Career Award. He was Associate Editor of Optics Express from 2004 to 2009, and he is currently the Chair of the Technical Committee for Photodetectors, Sensors, Systems and Imaging in the IEEE Photonics Society. Dr. Hayat is a Senior Member of IEEE and Member of the International Society for Optical Engineers and the Optical Society of America.